Mendeleev Communications

Mendeleev Commun., 2026, **36**, 25–27

Brightly emissive dinuclear silver(I) complexes based on a pyridine bisphosphine ligand

Maria P. Davydova,[a] Maria A. Trusova,[a,b] Valery K. Brel,[c]
Irina Yu. Bagryanskaya[d] and Alexander V. Artem'ev*[a]

[a] *A. V. Nikolaev Institute of Inorganic Chemistry, Siberian Branch of the Russian Academy of Sciences, 630090 Novosibirsk, Russian Federation. E-mail: chemisufarm@yandex.ru*
[b] *Department of Natural Sciences, Novosibirsk State University, 630090 Novosibirsk, Russian Federation*
[c] *A. N. Nesmeyanov Institute of Organoelement Compounds, Russian Academy of Sciences, 119334 Moscow, Russian Federation*
[d] *N. N. Vorozhtsov Novosibirsk Institute of Organic Chemistry, Siberian Branch of the Russian Academy of Sciences, 630090 Novosibirsk, Russian Federation*

DOI: 10.71267/mencom.7841

Dinuclear complexes [$Ag_2I_2L_2$] and [$Ag_2I_2L(PPh_3)_2$] were synthesized using 2,3-bis(diphenylphosphino)pyridine, a previously unexplored ligand. The second complex was isolated as solvates with $CHCl_3$ or Et_2O molecules possessing the same molecular geometry, but very different intramolecular Ag···Ag distances (3.630 and 3.098 Å, respectively). At room temperature, both complexes [$Ag_2I_2L_2$] and [$Ag_2I_2L(PPh_3)_2$] display strong blue-green luminescence with quantum yields of 32 and 62% and decay times of 6.9 and 12 μs, respectively.

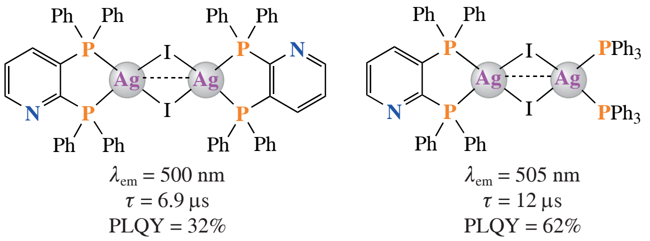

λ_{em} = 500 nm
τ = 6.9 μs
PLQY = 32%

λ_{em} = 505 nm
τ = 12 μs
PLQY = 62%

Keywords: 2,3-bis(diphenylphosphino)pyridine, silver(I) complexes, dinuclear complexes, luminescence, structure.

Silver(I) complexes have garnered significant interest due to their remarkable luminescent properties, catalytic activity, and biological[1,2] applications. These complexes also exhibit diverse structural motifs,[3–10] often featuring ligand-supported Ag···Ag metallophilic interactions[11] that can influence their emission characteristics. At room temperature, Ag^I complexes may display solid-state phosphorescence[12,13] or thermally activated delayed fluorescence (TADF),[14–16] with emissions arising from either intraligand (IL) or metal-to-ligand charge transfer (MLCT) processes. The specific emission mechanism depends on the complex structure and the nature of the supporting ligands.[17] For instance, Ag^I complexes coordinated with O-, N-, and S-donor ligands typically exhibit intraligand or cluster-centered phosphorescence,[18–21] whereas phosphine-based Ag^I complexes can demonstrate TADF.[14] Ligands containing a combination of 'hard' and 'soft' donor atoms have proven particularly effective for designing highly emissive organosilver(I) compounds. A notable example is the use of P,N-ligands such as 2-pyridylphosphines, which have enabled the synthesis of a series of promising silver(I)-based emitters.[22–25] Expanding the library of pyridylphosphine ligands in this field could thus lead to novel Ag^I complexes with intriguing structural and luminescent properties. Herein, we report dinuclear Ag^I iodide complexes supported by 2,3-bis(diphenylphosphino)pyridine **L**, a previously unexplored multidentate ligand.

As our experiments have shown, stoichiometric reaction of **L** with AgI in acetonitrile under stirring yields complex [$Ag_2I_2L_2$] **1** in a 88% isolated yield. When the reaction is performed in the presence of PPh_3 (AgI/**L**/PPh_3 = 2 : 1 : 2), complex [$Ag_2I_2L(PPh_3)_2$] **2** is obtained in a 72% yield. Crystallization of **2** from a $CHCl_3/Et_2O$ mixture produces a combination of solvates, **2**·$CHCl_3$ and **2**·Et_2O (Scheme 1).

Physically, compounds **1** and **2** are air-stable, colorless powders soluble in acetonitrile, chloroform, dichloromethane,

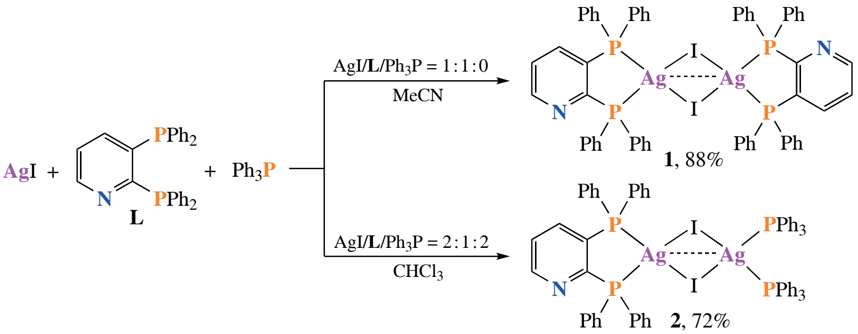

Scheme 1

and acetone. The phase purity of bulk **1** was confirmed by powder X-ray diffraction (PXRD, see Online Supplementary Materials, Figure S1) and elemental analysis. Solvates **2**$\cdot$CHCl$_3$ and **2**$\cdot$Et$_2$O readily lose solvent molecules to yield the non-solvated form **2** whose experimental PXRD pattern differs from those simulated for the solvated structures, as expected. The ^{1}H and ^{31}P{^{1}H} NMR spectra of **1** and **2** in solution are consistent with their formulations (Figures S2–S5). Specifically, the ^{31}P{^{1}H} NMR spectrum of **1** (Figure S4) displays two broad peaks corresponding to the two non-equivalent phosphorus atoms of ligand **L**. In the ^{31}P{^{1}H} NMR spectrum of **2**, the same peaks appear alongside a singlet attributed to the Ph$_3$P ligands (Figure S5).

The X-ray crystal structures of **1**, **2**$\cdot$CHCl$_3$ and **2**$\cdot$Et$_2$O are shown in Figure 1, with selected interatomic distances and angles listed in Table 1.† All structures feature a rhomboid Ag$_2$I$_2$ unit stabilized by either two **L** ligands (in **1**) or one **L** and two Ph$_3$P ligands (in **2**). In each case, the ligand **L** exhibits a *P*,*P*′-chelating coordination mode. The resulting AgP$_2$C$_2$ chelate rings adopt an envelope conformation, with the silver atom positioned at the apex. The Ag atoms display a distorted tetrahedral Ag@P$_4$ coordination geometry ($\tau_4 \approx 0.85$). The observed Ag–I (~2.8 Å) and Ag–P (2.48–2.56 Å) bond lengths agree with the literature values for related dinuclear Ag$^{\rm I}$ complexes.[30–34] Notably, the intramolecular Ag···Ag distance in **1** (3.29 Å) is significantly shorter than the sum of the van der Waals radii (3.44 Å),[35] suggesting argentophilic interactions.[36] A similar trend is observed in **2**$\cdot$Et$_2$O, where the Ag···Ag distance (3.098 Å, 90% ΣrvdW) is even shorter than that in **1**. In contrast, **2**$\cdot$CHCl$_3$ exhibits a longer Ag···Ag separation (3.630 Å, 105% ΣrvdW), indicating the absence of metallophilic bonding. Thus, despite nearly identical molecular geometries in solvates **2**$\cdot$CHCl$_3$ and **2**$\cdot$Et$_2$O, the Ag···Ag distance varies dramatically. This unexpected sensitivity of these distances to the solvate arrangement highlights a pronounced structural flexibility in **2**.

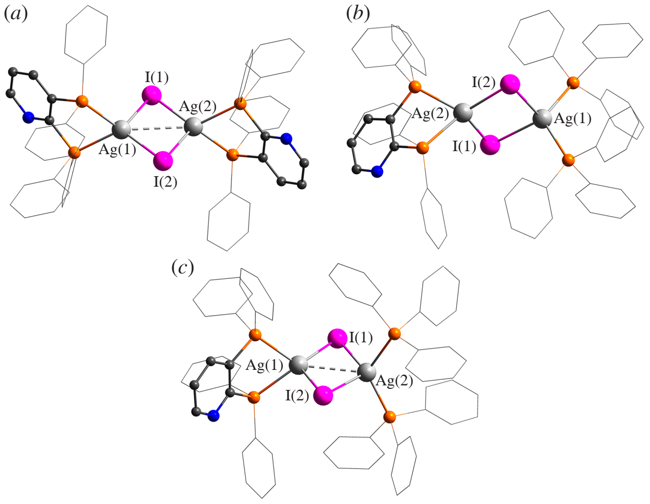

Figure 1 X-ray derived structures of (*a*) complex **1**, (*b*) solvate **2**$\cdot$CHCl$_3$, and (*c*) solvate **2**$\cdot$Et$_2$O. The solvent molecules and H atoms are omitted for clarity.

To investigate the stereoelectronic structures of **1** and **2** in the gas phase, DFT calculations were performed at the PBE0-D3(BJ)/LANL2DZ/6-31+G(d,p) level of theory (see Online Supplementary Materials for details). Interestingly, the optimized structures of **1** and **2** deviate significantly from their X-ray geometries. The Ag$_2$I$_2$ core in the optimized structures adopts a butterfly-shaped conformation, with Ag···Ag distances 12.9 and 20% shorter than those in the X-ray structures (2.86 and 2.90 Å). The highest occupied molecular orbitals (HOMOs) of both complexes are primarily contributed by Ag d-orbitals, I p-orbitals, and P p-orbitals (Figures S8, S9). The lowest unoccupied molecular orbitals (LUMOs) consist exclusively of pyridine π-orbitals. Notably, such HOMO/LUMO distribution patterns are nearly identical for the calculated X-ray geometries of **1** and **2**. These results suggest that the low-energy excited states of both complexes are likely of (M + X)LCT character.

At ambient temperature, polycrystalline samples **1** and **2** show strong blue-green photoluminescence (PL). Their excitation and emission spectra at ambient temperature are shown in Figure 2. The emission profiles adopt a broad shape

Table 1 Selected interatomic distances (Å) and angles (deg).

Sample	Distances/Å			Angles/deg		
	Ag–I	Ag–P	Ag···Ag	Ag–I–Ag	I–Ag–I	I–Ag–P
1	2.7914(5), 2.8386(5)	2.5357(13), 2.5491(14)	3.2874(7)	71.446(14), 71.446(14)	108.554(14), 108.554(14)	111.19(3)–123.99(4)
2$\cdot$CHCl$_3$	2.7381(10)–2.9831(10)	2.512(3)–2.561(3)	3.630(9)	78.33(3), 78.71(3)	98.14(3), 104.71(3)	103.27(6)–129.54(6)
2$\cdot$Et$_2$O	2.7703(8)–2.9239(8)	2.4855(12)–2.5601(10)	3.0976(6)	64.780(9), 65.909(9)	111.173(11), 117.854(11)	103.99(3)–124.48(3)

---

† Crystals of **1** were grown by slow evaporation of a MeCN solution of **1** at 23 °C for 24 h. The free solvent accessible volume in **1** derived from PLATON[26,27] routine analysis was found to be 9.75% (135.0 Å^3). This volume is occupied by disordered solvent molecules of the MeCN (one molecule in the independent part of the unit cell). We employed the PLATON/SQUEEZE procedure to calculate the contribution to the diffraction from the solvent region and thereby produced a set of solvent-free diffraction intensities.

Crystal data for **1**. C$_{58}$H$_{46}$Ag$_2$I$_2$N$_2$P$_4$, $M = 1364.39$, triclinic space group $P\bar{1}$, 200 K, $a = 10.7256(6)$, $b = 11.4671(6)$ and $c = 12.1850(6)$ Å, $\alpha = 97.031(2)°$, $\beta = 103.970(2)°$, $\gamma = 103.970(2)°$, $Z = 1$, $V = 1385.09(13)$ Å^3. The crystal with dimensions 0.20×0.10×0.02 mm was selected and intensities with 16457 reflections were measured. μ(MoK$_\alpha$) = 1.98 mm^{-1}, $R_{\rm int} = 0.037$, which were used in all calculations. The final R_1 was 0.041 [$F^2 > 2\sigma(F^2)$] and $wR(F^2)$ was 0.084.

Crystals of **2**$\cdot$CHCl$_3$ and **2**$\cdot$Et$_2$O were grown by vapour diffusion of Et$_2$O into the CHCl$_3$ solution at 23 °C for 24 h.

Crystal data for **2**$\cdot$CHCl$_3$. C$_{66}$H$_{54}$Ag$_2$Cl$_3$I$_2$NP$_4$, $M = 1560.87$, monoclinic space group $P2_1/c$, 296 K, $a = 23.8555(18)$, $b = 15.5309(12)$ and $c = 18.2994(15)$ Å, $\beta = 109.598(4)°$, $Z = 4$, $V = 6387.1(9)$ Å^3. The crystal with dimensions 0.30×0.20×0.03 mm was selected and intensities with 42222 reflections were measured. μ(MoK$_\alpha$) = 1.85 mm^{-1}, $R_{\rm int} = 0.097$, which were used in all calculations. The final R_1 was 0.066 [$F^2 > 2\sigma(F^2)$] and $wR(F^2)$ was 0.165.

Crystal data for **2**$\cdot$Et$_2$O. C$_{69}$H$_{63}$Ag$_2$I$_2$NOP$_4$, $M = 1515.62$, monoclinic space group $P2_1/c$, 296 K, $a = 23.214(7)$, $b = 12.360(3)$ and $c = 23.965(6)$ Å, $\beta = 108.840(8)°$, $Z = 4$, $V = 6508(3)$ Å^3. The crystal with dimensions 0.50×0.15×0.05 mm was selected and intensities with 49431 reflections were measured. μ(MoK$_\alpha$) = 1.69 mm^{-1}, $R_{\rm int} = 0.074$, which were used in all calculations. The final R_1 was 0.038 [$F^2 > 2\sigma(F^2)$] and $wR(F^2)$ was 0.097.

The data for **1**, **2**$\cdot$CHCl$_3$ and **2**$\cdot$Et$_2$O were collected on a Bruker Kappa Apex II CCD diffractometer using φ,ω-scans of narrow (0.5°) frames with MoKα radiation ($\lambda = 0.71073$ Å) and a graphite monochromator. The structures were solved by direct methods SHELXL97 and refined by a full matrix least-squares anisotropic–isotropic (for H atoms) procedure using the SHELXL-2014/7 program set.[28] Absorption corrections were applied using the empirical multiscan method with the SADABS program.[29] The positions of the hydrogen atoms were calculated with the riding model.

CCDC 2446309–2446311 contain the supplementary crystallographic data for this paper. These data can be obtained free of charge from The Cambridge Crystallographic Data Center at https://www.ccdc.cam.ac.uk.

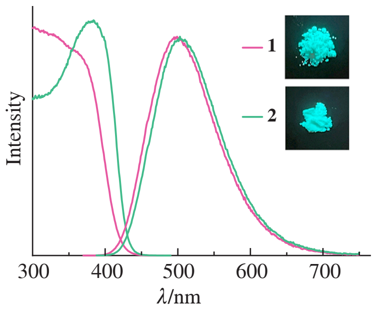

Figure 2 Normalized excitation (λ_{em} = 500 nm for **1** and λ_{em} = 505 nm for **2**) and emission spectra (λ_{ex} = 360 nm for **1** and λ_{ex} = 380 nm for **2**) recorded at 298 K. Insets show PL of the solid samples under 365 nm light.

with maxima at 500 (**1**) and 505 nm (**2**). No excitation-dependent behavior is observed for these compounds. At that temperature, the photoluminescence quantum yields (PLQYs) of **1** and **2** are 32 and 62%, and the PL times are 6.9 and 12 µs, respectively. Taking into account these data and the results of DFT calculations, the PL of **1** and **2** can be tentatively assigned to phosphorescence or TADF of (M + X)LCT type.

In summary, the reaction of 2,3-bis(diphenylphosphino)pyridine **L** with AgI yields a bridging dimer [$Ag_2I_2L_2$] **1**, whereas the AgI/**L**/Ph_3P system forms a non-symmetric complex [$Ag_2I_2L(PPh_3)_2$] **2**. The latter was isolated as solvates (**2**$\cdot CHCl_3$ and **2**$\cdot Et_2O$), which exhibit similar molecular geometries but significantly different intramolecular Ag···Ag distances (3.630 *vs*. 3.098 Å). Both complexes display bright blue-green photoluminescence of (M + X)LCT character, with moderate-to-high quantum yields and microsecond lifetimes.

This work was supported by the Ministry of Science and Higher Education of the Russian Federation (contract no. 075-00276-75-00). The authors thank Dr. M. I. Rakhmanova for recording PL spectra as well as the Center of Collective Use of NIOC SB RAS for the opportunity to obtain X-ray diffraction data and the Center for Molecular Composition Studies of INEOS RAS.

Online Supplementary Materials

Supplementary data associated with this article can be found in the online version at doi: 10.71267/mencom.7841.

References

1 M. F. Galimova, K. A. Burdina, A. B. Dobrynin, A. P. Lyubina, A. D. Voloshina, E. I. Musina and A. A. Karasik, *Inorg. Chim. Acta*, 2024, **563**, 121896; https://doi.org/10.1016/j.ica.2023.121896.

2 A. V. Artem'ev, J. A. Eremina, E. V. Lider, O. V. Antonova, E. V. Vorontsova and I. Yu. Bagryanskaya, *Polyhedron*, 2017, **138**, 218; https://doi.org/10.1016/j.poly.2017.09.041.

3 A. A. Shmakova, A. S. Berezin, P. A. Abramov and M. N. Sokolov, *Inorg. Chem.*, 2020, **59**, 1853; https://doi.org/10.1021/acs.inorgchem.9b03064.

4 A. V. Golubev, A. S. Kubasov, E. A. Malinina, S. E. Nikiforova, L. V. Goeva, V. V. Avdeeva, A. Yu. Bykov, K. Yu. Zhizhin and N. T. Kuznetsov, *Inorg. Chim. Acta*, 2024, **573**, 122344; https://doi.org/10.1016/j.ica.2024.122344.

5 A. V. Golubev, A. S. Kubasov, E. A. Malinina, S. E. Nikiforova, L. V. Goeva, V. V. Avdeeva, A. Yu. Bykov, R. A. Novikov, K. Yu. Zhizhin and N. T. Kuznetsov, *Cryst. Growth Des.*, 2024, **24**, 3319; https://doi.org/10.1021/acs.cgd.4c00049.

6 V. I. Komlyagina, N. F. Romashev, V. V. Kokovkin, A. L. Gushchin, E. Benassi, M. N. Sokolov and P. A. Abramov, *Molecules*, 2022, **27**, 6961; https://doi.org/10.3390/molecules27206961.

7 A. V. Chupina, V. V. Yanshole, V. S. Sulyaeva, V. V. Kokovkin, P. A. Abramov and M. N. Sokolov, *Dalton Trans.*, 2022, **51**, 705; https://doi.org/10.1039/D1DT02398E.

8 V. I. Komlyagina, I. V. Bakaev, N. F. Romashev and A. L. Gushchin, *Chem. – Asian J.*, 2025, **20**, e202401455; https://doi.org/10.1002/asia.202401455.

9 E. S. Vikulova, T. S. Sukhikh, A. S. Barysheva, I. Y. Ilyin, D. P. Pishchur and N. B. Morozova, *J. Struct. Chem.*, 2024, **65**, 489; https://doi.org/10.1134/S0022476624030065.

10 Ya. V. Demyanov, I. Yu. Bagryanskaya and A. V. Artem'ev, *Mendeleev Commun.*, 2024, **34**, 812; https://doi.org/10.1016/j.mencom.2024.10.014.

11 A. Olbrykh, G. Yakovlev, A. Titov and E. Shubina, *Crystals*, 2025, **15**, 115; https://doi.org/10.3390/cryst15020115.

12 M. Z. Shafikov, R. Czerwieniec and H. Yersin, *Dalton Trans.*, 2019, **48**, 2802; https://doi.org/10.1039/C8DT04078H.

13 M. I. Rogovoy, M. I. Rakhmanova, E. H. Sadykov, G. M. Carignan, I. Yu. Bagryanskaya, J. Li and A. V. Artem'ev, *Chem. Commun.*, 2023, **59**, 11413; https://doi.org/10.1039/D3CC03540A.

14 H. Yersin, R. Czerwieniec, M. Z. Shafikov and A. F. Suleymanova, *ChemPhysChem*, 2017, **18**, 3508; https://doi.org/10.1002/cphc.201700872.

15 A. V. Artem'ev, M. I. Rogovoy, I. M. Odud, M. P. Davydova, M. I. Rakhmanova, P. A. Petrov, V. K. Brel, O. I. Artushin, K. A. Brylev, D. G. Samsonenko, A. S. Berezin, D. E. Gorbunov and N. P. Gritsan, *Inorg. Chem. Front.*, 2024, **11**, 8778; https://doi.org/10.1039/D4QI01996B.

16 M. Z. Shafikov, A. F. Suleymanova, R. Czerwieniec and H. Yersin, *Inorg. Chem.*, 2017, **56**, 13274; https://doi.org/10.1021/acs.inorgchem.7b02002.

17 N. A. Shekhovtsov, K. A. Vinogradova, A. S. Berezin, T. S. Sukhikh, V. P. Krivopalov, E. B. Nikolaenkova and M. B. Bushuev, *Inorg. Chem. Front.*, 2020, **7**, 2212; https://doi.org/10.1039/D0QI00254B.

18 V. V. Volchek, A. S. Berezin, M. N. Sokolov and P. A. Abramov, *Inorganics*, 2022, **10**, 225; https://doi.org/10.3390/inorganics10120225.

19 A. P. Olbrykh, A. V. Tsorieva, V. M. Korshunov, A. F. Smol'yakov, I. A. Godovikov, A. A. Korlykov, I. V. Taydakov, A. A. Titov, O. A. Filippov and E. S. Shubina, *Inorg. Chem. Front.*, 2025, **12**, 812; https://doi.org/10.1039/D4QI02624A.

20 K. F. Baranova, A. A. Titov, J. R. Shakirova, V. A. Baigildin, A. F. Smol'yakov, D. A. Valyaev, G.-H. Ning, O. A. Filippov, S. P. Tunik and E. S. Shubina, *Inorg. Chem.*, 2024, **63**, 16610; https://doi.org/10.1021/acs.inorgchem.4c00751.

21 T. S. Sukhikh, D. A. Bashirov, S. Shuvaev, V. Yu. Komarov, N. V. Kuratieva, S. N. Konchenko and E. Benassi, *Polyhedron*, 2018, **141**, 77; https://doi.org/10.1016/j.poly.2017.11.017.

22 A. V. Shamsieva, E. I. Musina, T. P. Gerasimova, R. R. Fayzullin, I. E. Kolesnikov, A. I. Samigullina, S. A. Katsyuba, A. A. Karasik and O. G. Sinyashin, *Inorg. Chem.*, 2019, **58**, 7698; https://doi.org/10.1021/acs.inorgchem.8b03474.

23 J. Elistratova, B. Faizullin, A. Shamsieva, T. Gerasimova, I. V. Kashnik, K. A. Brylev, V. Babaev, K. Kholin, I. Nizameev, E. Musina, S. Katsyuba, A. Karasik, O. Sinyashin and A. Mustafina, *J. Mol. Liq.*, 2020, **305**, 112853; https://doi.org/10.1016/j.molliq.2020.112853.

24 A. Yu. Baranov, M. I. Rakhmanova, D. G. Samsonenko, S. F. Malysheva, N. A. Belogorlova, I. Yu. Bagryanskaya, V. P. Fedin and A. V. Artem'ev, *Inorg. Chim. Acta*, 2019, **494**, 78; https://doi.org/10.1016/j.ica.2019.05.015.

25 A. V. Artem'ev, M. R. Ryzhikov, A. S. Berezin, I. E. Kolesnikov, D. G. Samsonenko and I. Yu. Bagryanskaya, *Inorg. Chem. Front.*, 2019, **6**, 2855; https://doi.org/10.1039/C9QI00657E.

26 A. L. Spek, *PLATON*, *Version 10M*, Utrecht, The Netherlands, 2003; https://www.platonsoft.nl/platon.

27 A. L. Spek, *J. Appl. Crystallogr.*, 2003, **36**, 7; https://doi.org/10.1107/S0021889802022112.

28 G. M. Sheldrick, *Acta Crystallogr.*, 2015, **C71**, 3; https://doi.org/10.1107/S2053229614024218.

29 *SADABS*, *Version 2008-1*, Bruker AXS, Madison, WI, USA, 2008.

30 L.-G. Yang, C.-C. Zhu, D.-P. Zhang, D.-C. Li, D.-Q. Wang and J.-M. Dou, *Polyhedron*, 2011, **30**, 1469; https://doi.org/10.1016/j.poly.2011.02.052.

31 G. Besenyei, G. Szalontai and L. Párkányi, *Polyhedron*, 2017, **127**, 97; https://doi.org/10.1016/j.poly.2017.01.048.

32 D. Freudenmann and C. Feldmann, *Inorg. Chim. Acta*, 2011, **375**, 311; https://doi.org/10.1016/j.ica.2011.05.006.

33 X. Li, S.-Y. Wei, D.-H. Zhang, J.-X. Hu, C.-L. Hou, T.-T. Lin, X.-L. Chen and C.-Z. Lu, *Dalton Trans.*, 2025, **54**, 1703; https://doi.org/10.1039/D4DT02855D.

34 E. Effendy, C. Di Nicola, M. Fianchini, C. Pettinari, B. W. Skelton, N. Somers and A. H. White, *Inorg. Chim. Acta*, 2005, **358**, 763; https://doi.org/10.1016/j.ica.2004.09.047.

35 A. Bondi, *J. Phys. Chem.*, 1964, **68**, 441; https://doi.org/10.1021/j100785a001.

36 M. Jansen, *Angew. Chem., Int. Ed.*, 1987, **26**, 1098; https://doi.org/10.1002/anie.198710981.

Received: 6th June 2025; Com. 25/7841